

Atmospheric Chemistry of 1,3-Dioxolane: Kinetic, Mechanistic, and Modeling Study of OH Radical Initiated Oxidation

C. G. Sauer, I. Barnes,* K. H. Becker, and H. Geiger

Bergische Universität GH Wuppertal/FB 9—Physikalische Chemie, Gausstrasse 20,
D-42119 Wuppertal, Germany

T. J. Wallington* and L. K. Christensen

Ford Motor Company, 20000 Rotunda Drive, Mail Drop SRL-3083, Dearborn, Michigan 48121-2053

J. Platz and O. J. Nielsen

Atmospheric Chemistry, Plant Biology and Biogeochemistry Department, Risø National Laboratory,
DK-4000, Roskilde, Denmark

Received: March 24, 1999; In Final Form: June 1, 1999

An absolute rate pulse radiolysis technique was used to measure $k(\text{OH} + 1,3\text{-dioxolane}) = (8.8 \pm 0.9) \times 10^{-12} \text{ cm}^3 \text{ molecule}^{-1} \text{ s}^{-1}$ at 295 K in 1000 mbar of Ar. Relative rate techniques were used to study the reactions of OH radicals and Cl atoms with 1,3-dioxolane and Cl atoms with ethylene carbonate and methylene glycol diformate at 300 K in 1 bar of synthetic air. Rate coefficients were $k(\text{OH} + 1,3\text{-dioxolane}) = (1.04 \pm 0.16) \times 10^{-11}$, $k(\text{Cl} + 1,3\text{-dioxolane}) = (1.6 \pm 0.3) \times 10^{-10}$, $k(\text{Cl} + \text{ethylene carbonate}) = (7.1 \pm 1.7) \times 10^{-12}$, and $k(\text{Cl} + \text{methylene glycol diformate}) = (5.6 \pm 0.7) \times 10^{-13} \text{ cm}^3 \text{ molecule}^{-1} \text{ s}^{-1}$. OH radical and chlorine atom initiated oxidation of 1,3-dioxolane in 1 bar of N_2/O_2 mixtures at 298 K in the presence of NO_x gives ethylene carbonate and methylene glycol diformate. Molar yields of ethylene carbonate and methylene glycol diformate were 0.48 ± 0.07 and 0.50 ± 0.14 for OH radical initiation and 0.43 ± 0.07 and 0.53 ± 0.07 for Cl atom initiation. Product yields were independent of O_2 partial pressure over the range studied (60–800 mbar). A photochemical mechanism was developed to describe the OH-initiated degradation of 1,3-dioxolane in the presence of NO_x . The results are discussed with respect to the available literature data concerning the atmospheric chemistry of ethers.

1. Introduction

Ethers are an important class of automotive fuel additives. For example, methyl *tert*-butyl ether (MTBE), ethyl *tert*-butyl ether (ETBE), *tert*-amyl methyl ether (TAME), and diisopropyl ether (DIPE) are widely used octane-enhancing additives in gasoline. In addition, ethers such as dimethyl ether¹ and dimethoxy methane are under consideration as alternative diesel fuels. To predict the environmental impact of ether fuels and fuel additives, it is desirable to understand how the structure of such molecules impacts their atmospheric reactivity and degradation pathways. While 1,3-dioxolane is not used currently as an automotive fuel additive, it is used as an industrial solvent. 1,3-Dioxolane is a convenient model compound whose chemistry provides insight into the behavior of alkyl peroxy and alkoxy radicals connected to oxygen ether linkages.

As for most chemicals released into the troposphere, the major atmospheric fate of 1,3-dioxolane will be reaction with OH radicals. We report here the results of a collaborative experimental study of the kinetics and mechanism of the OH radical initiated oxidation of 1,3-dioxolane.

Mechanistic studies are often limited to the detection of the primary reaction products. Reaction mechanisms, which are derived from these data, have not usually been subject to

validation by comparison of the measured product concentrations against model simulations. In other instances, where no suitable experimental results are available, reaction mechanisms are postulated without any further verification. Both methods result in the transfer of considerable uncertainty to the results of models when applied, e.g., to the modeling of field data. As a consequence, this work also includes the development of an explicit photochemical degradation mechanism, which was constructed by using the results obtained from the photoreactor experiments. The reaction scheme was validated by comparison of simulated and experimental concentration/time profiles.

Altogether, the present work provides an intensive kinetic, product, and modeling study on the OH-initiated oxidation of 1,3-dioxolane.

2. Experimental Section

Four experimental systems were used.^{2–5} They are described briefly here.

2.1. Pulse Radiolysis System at Risø National Laboratory. To study the reaction between OH radicals and 1,3-dioxolane,



OH radicals were generated from H_2O by pulsed radiolysis of Ar/ H_2O gas mixtures in a 1 L stainless steel reaction cell with a 30 ns pulse of 2 MeV electrons from a Febetron 705 field

* To whom correspondence should be addressed. E-mail: barnes@physchem.uni-wuppertal.de. E-mail: twalling@ford.com.

emission accelerator². Ar diluent was always in great excess and was used to generate Ar* atoms as follows:



The radiolysis dose was varied by insertion of stainless steel attenuators between the accelerator and the reaction cell. OH radicals were monitored using their characteristic absorption at 309.25 nm. The initial OH concentration was approximately 10^{13} cm^{-3} . The analysis light was provided by a pulsed 150 W Xenon arc lamp and was multipassed through the reaction cell using internal White cell optics to give a total optical path length of 120 cm. After leaving the cell, the light was guided through a monochromator (operated with a spectral resolution of 1 nm) and detected by a photomultiplier. All absorption transients were derived from single pulse experiments.

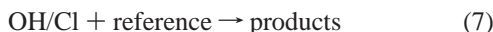
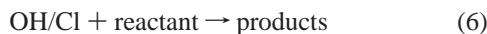
Reagent purities and concentrations were as follows: Ar (ultrahigh purity) 980–990 mbar; H₂O (triple distilled deionized water) 5–15 mbar; 1,3-dioxolane (>99%) 0.8–2.4 mbar. All experiments were performed at $295 \pm 2 \text{ K}$ and 1000 mbar total pressure. 1,3-Dioxolane was degassed by freeze–pump–thaw cycling before use, all other reagents were used as received.

2.2. FTIR–Smog Chamber System at Wuppertal. The majority of experiments were performed in a 1080 L quartz photoreactor surrounded by 32 fluorescent lamps (Philips TL05/40 W) and 32 mercury lamps (Philips TUV/40 W)³. A multireflection White mirror system (484.7 m optical path length) mounted in the reactor and coupled to a Fourier transform infrared (FTIR) spectrometer Bruker IFS-88 allowed in situ monitoring of both reactants and products. Additional experiments were carried out in a 20 L glass photoreactor surrounded by four fluorescent lamps.⁴

Relative rate kinetic experiments were performed in synthetic air or nitrogen at total pressures of $1000 \pm 40 \text{ mbar}$ at $300 \pm 4 \text{ K}$. OH radicals were generated by the photolysis of hydrogen peroxide using mercury lamps; Cl atoms were generated by the photolysis of Cl₂ using fluorescent lamps.



Provided that the reactant and the reference compound are removed solely by the reaction of interest and are not reformed in any process,



it can be shown that

$$\ln \frac{[\text{reactant}]_{t_0}}{[\text{reactant}]_t} = \frac{k_6}{k_7} \ln \frac{[\text{reference}]_{t_0}}{[\text{reference}]_t}$$

where $[\text{reactant}]_{t_0}$ and $[\text{reactant}]_t$ and $[\text{reference}]_{t_0}$ and $[\text{reference}]_t$ are the reactant and reference concentrations at times t_0 and t , respectively, and k_6 and k_7 are the rate coefficients for reactions 6 and 7. A plot of $\ln([\text{reactant}]_{t_0}/[\text{reactant}]_t)$ versus $\ln([\text{reference}]_{t_0}/[\text{reference}]_t)$ yields a slope of k_6/k_7 . When there is an additional loss process for the reactant,



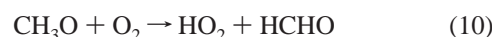
the data can be analyzed using the following expression:⁶

$$\ln \frac{[\text{reactant}]_{t_0}}{[\text{reactant}]_t} - k_8 t = \frac{k_6}{k_7} \ln \frac{[\text{reference}]_{t_0}}{[\text{reference}]_t}$$

where k_8 is the rate coefficient for reaction 8.

Reagent compounds were injected into the reactor in a stream of synthetic air using microliter syringes or gastight syringes. Ethylene carbonate is a solid and was introduced into the chamber by heating and evaporating a known mass of the compound into a stream of synthetic air. Initial concentrations were in the range 0.1–20 ppm (1 ppm = $2.46 \times 10^{13} \text{ molecules cm}^{-3}$). In the 20 L photoreactor, initial concentrations were about 1 order of magnitude higher. Samples were taken from the small reactor with a gastight syringe and analyzed by GC/FID (gas chromatograph HP 5890, RTx1 capillary column 30 m \times 0.53 mm \times 1 μm or m-AT 1701 capillary column 30 m \times 0.53 mm \times 1.2 μm , electronic integrator HP 3396).

Product studies were performed in the 1080 L quartz photoreactor at $298 \pm 4 \text{ K}$ and $1000 \pm 20 \text{ mbar}$ total pressure of synthetic air or O₂/N₂ mixtures with different O₂ partial pressures in the range 60–800 mbar. Photolysis of methyl nitrite in the presence of NO was used as an OH source.

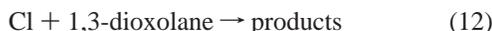


The photolysis of chlorine, reaction 5, served as a source for Cl atoms. Initial concentrations were 2.8–4.9 ppm of 1,3-dioxolane, 2–20 ppm of methyl nitrite, 1–5 ppm of NO, and 1–5 ppm of Cl₂. Individual experiments lasted 5–23 min in which time 10 FTIR spectra (32 or 64 scans, 1 cm^{-1} spectral resolution) were collected. After irradiation, another 10 spectra were collected to determine the wall loss rate of ethylene carbonate.

1,3-Dioxolane (Aldrich, 99.9%), ethylene carbonate (Aldrich, 98%), cyclohexane (Aldrich, 99.9%), dichloromethane (Aldrich, HPLC grade), and hydrogen peroxide (Peroxid Chemie, 85%) were used without further purification. Methyl nitrite was synthesized by the dropwise addition of concentrated sulfuric acid to a saturated solution of sodium nitrite in methanol. The gaseous methyl nitrite was passed over solid calcium chloride, collected in an ethanol/dry ice cold trap, and stored at $-78 \text{ }^\circ\text{C}$ in the dark. FT-IR analysis showed neither methanol nor water. Methylene glycol diformate was prepared from ethylene carbonate in a five-step synthesis^{7–10} and was handled as a solution in dichloromethane or deuteriochloromethane. The following spectroscopic data were obtained. ¹H NMR (400 MHz, CDCl₃): $\delta(\text{ppm}) = 5.91 \text{ (s, 2H)}, 8.09 \text{ (s, 2H)}$. IR, gas (cm^{-1}): 2949, 1769, 1168, 1096, 957. No impurities were observed. All gases were supplied by Messer Griesheim and had the following stated purities in vol %: synthetic air (99.995), N₂ (99.999), O₂ (99.995), NO (99.8), NO₂ (98), Cl₂ (99.8), methane (99.995), ethane (99.95), propane (99.95), *n*-butane (99.5), chloroethane (99.0).

2.3. FTIR–Smog Chamber System at Ford Motor Company. Experiments were performed in a 140 L Pyrex reactor interfaced to a Mattson Sirius 100 FTIR spectrometer.⁵ The reactor was surrounded by 22 fluorescent blacklamps (GE F15T8-BL). Loss of 1,3-dioxolane and formation of products were monitored by FTIR spectroscopy using an infrared path length of 28 m and a resolution of 0.25 cm^{-1} . Infrared spectra were derived from 32 co-added interferograms.

The products of the reaction of 1,3-dioxolane and Cl atoms,



were investigated by irradiating 1,3-dioxolane/Cl₂/NO/O₂/N₂ mixtures at 296 ± 2 K. Initial concentrations of the gas mixtures were 17–37 mTorr of 1,3-dioxolane, 96–148 mTorr of Cl₂, 16–43 mTorr of NO, and 77–600 Torr of O₂ in 700 Torr (760 Torr = 1013 mbar) total pressure of N₂ diluent. A reference spectrum of ethylene carbonate was acquired by introducing vapor from a commercial sample into the chamber. Ethylene carbonate has a vapor pressure at room temperature of approximately 25 mTorr. It is difficult to measure such low pressures with great accuracy, and absolute calibration of the spectrum was achieved using the infrared cross sections measured at Wuppertal. A reference spectrum of methylene glycol diformate was generated from irradiation of 1,3,5-trioxane/Cl₂/O₂/N₂ mixtures¹¹ and calibrated using the infrared cross section measured at Wuppertal.

In smog chamber experiments, unwanted loss of reactants and products via photolysis, dark chemistry, and wall reactions have to be considered. Control experiments were performed to check for such unwanted losses in the chamber. No significant loss of 1,3-dioxolane (<1%) due to photolysis was observed. No significant loss of 1,3-dioxolane (<2%) or methylene glycol diformate (<2%) was observed when mixtures of these compounds in air were left in the dark for 7–45 min, showing that heterogeneous loss of 1,3-dioxolane and methylene glycol diformate in the chamber are not important. When gas mixtures containing ethylene carbonate were allowed to stand in the dark, a slow loss of this compound was observed (with first-order rate constants of 0.01–0.03 min⁻¹) presumably due to deposition on the reactor walls.

3. Results

3.1. Pulse Radiolysis Study of Reaction of OH Radicals with 1,3-Dioxolane at Risø. A rapid increase in absorption was observed 0–1 μs after the radiolysis pulse which was attributed to the formation of OH radicals, which absorb strongly at 309.25 nm. The subsequent decay of absorption followed first-order kinetics and is ascribed to loss of OH radicals via reaction with 1,3-dioxolane. All transients were well described using the following expression:

$$[\text{OH}]_t = [\text{OH}]_0 \exp(-k^{1st}t)$$

where [OH]_t and [OH]₀ are the OH radical concentrations at time *t* and time 0 and *k*^{1st} is the first-order rate constant of reaction 1. Figure 1 shows a plot of *k*^{1st} versus the 1,3-dioxolane concentration. Linear least-squares regression of the data in Figure 1 gives *k*₁ = (8.8 ± 0.8) × 10⁻¹² cm³ molecule⁻¹ s⁻¹. To account for additional uncertainties associated with the nonlinear relationship between [OH] and the UV absorption at 309.25 nm,¹² we choose to propagate an additional 5% uncertainty range and obtain a final value of *k*₁ = (8.8 ± 0.9) × 10⁻¹² cm³ molecule⁻¹ s⁻¹.

3.2. Relative Rate Study of Reaction of OH Radicals with 1,3-Dioxolane at Wuppertal. The kinetics of reaction 1 were studied using *n*-butane and cyclohexane as reference compounds.

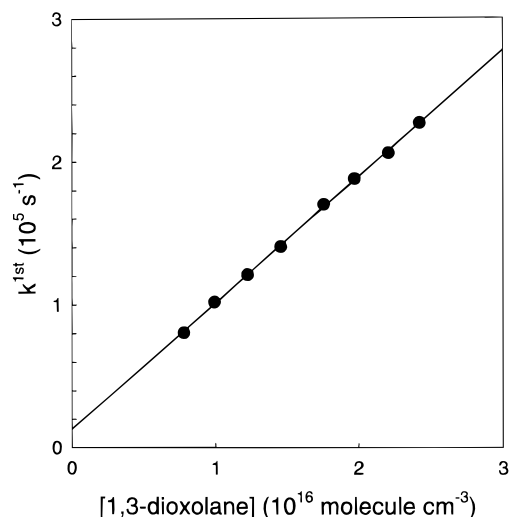


Figure 1. Pseudo-first-order loss of OH radicals versus 1,3-dioxolane concentration.

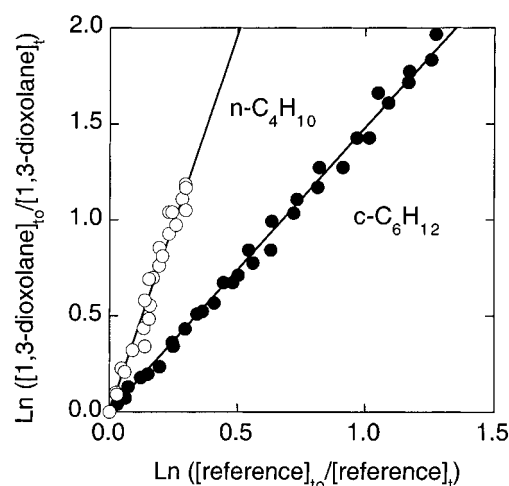
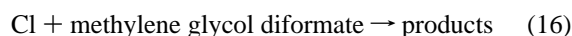
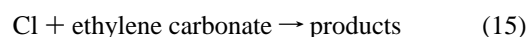
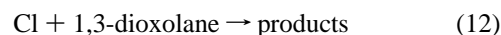


Figure 2. Decay of 1,3-dioxolane versus *n*-C₄H₁₀ and *c*-C₆H₁₂ when exposed to OH radicals in 1000 mbar total pressure of air at 300 K.

The kinetics of reactions 13 and 14 are well established. In 1 atm of air diluent at 296 K, *k*₁₃ = 2.44 × 10⁻¹² and *k*₁₄ = 7.49 × 10⁻¹² cm³ molecule⁻¹ s⁻¹.¹³ Figure 2 shows plots of the loss of 1,3-dioxolane versus those of *n*-C₄H₁₀ and cyclohexane. Linear least-squares analysis gives *k*₁/*k*₁₃ = 3.96 ± 0.32 and *k*₁/*k*₁₄ = 1.50 ± 0.08. Hence, values of *k*₁ = (9.66 ± 0.78) × 10⁻¹² and (1.12 ± 0.06) × 10⁻¹¹ cm³ molecule⁻¹ s⁻¹ are derived. Consistent results were obtained using the two different reference compounds. We choose to quote the average of the results above with error limits which encompass the extremes of the ranges, hence *k*₁ = (1.04 ± 0.16) × 10⁻¹¹ cm³ molecule⁻¹ s⁻¹. This result is indistinguishable, within the experimental uncertainties, from that of *k*₁ = (8.8 ± 0.9) × 10⁻¹² cm³ molecule⁻¹ s⁻¹ measured using the pulse radiolysis technique described in the previous section.

3.3. Cl Atom Relative Rate Studies at Wuppertal and Ford. Relative rate experiments were performed to investigate the kinetics of the reactions of Cl atoms with 1,3-dioxolane, ethylene carbonate, and methylene glycol diformate.



The kinetics of reaction 12 were measured relative to reactions

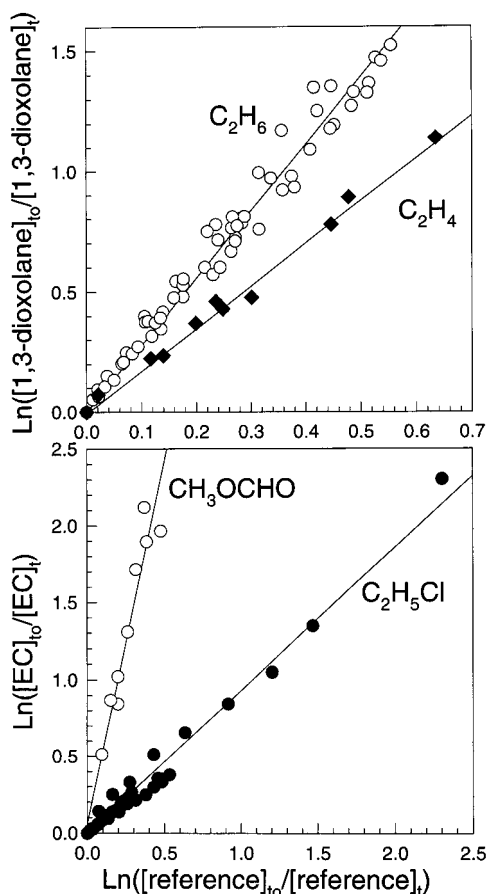
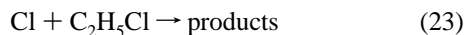
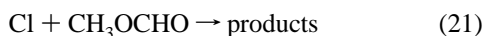


Figure 3. Decay of 1,3-dioxolane versus C_2H_4 and C_2H_6 (top) and ethylene carbonate (EC, corrected for wall loss) versus C_2H_5Cl and CH_3OCHO (bottom) when exposed to Cl atoms at 300 K.

18–20, reaction 15 was studied relative to (21) and (23), and reaction 16 was compared to (17) and (22).



Representative results obtained at Wuppertal and Ford using 1,3-dioxolane and ethylene carbonate as reactants and C_2H_6 , C_2H_4 , CH_3OCHO , and C_2H_5Cl as references are shown in Figure 3. The ethylene carbonate decay was corrected for wall loss as described in section 2.2. Linear least-squares analyses of the data shown in Figure 3 and analogous plots give the rate constant ratios shown in Table 1. Indicated errors are two standard deviations of the linear regression.

The rate constant ratios in Table 1 can be placed upon an absolute basis using $k_{17} = 1.0 \times 10^{-13}$,¹⁴ $k_{18} = 5.7 \times 10^{-11}$,¹⁴ $k_{19} = 1.4 \times 10^{-10}$,¹⁴ $k_{20} = 9.4 \times 10^{-11}$,¹⁴ $k_{21} = 1.4 \times 10^{-12}$,¹⁵ $k_{22} = 3.3 \times 10^{-13}$,¹⁴ and $k_{23} = 8.0 \times 10^{-12}$,¹⁶ to give the data in Table 2. Consistent results were obtained using the different reference compounds. We choose to quote values for k_{12} , k_{15} , and k_{16} which are averages of the results in Table 2 with error limits which encompass the extremes of the ranges, hence k_{12}

TABLE 1: Measured Cl Atom Rate Constant Ratios

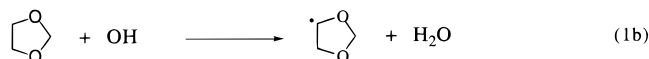
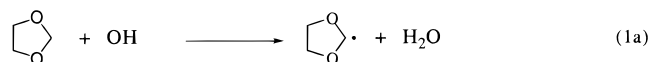
reference	reactant		
	1,3-dioxolane	ethylene carbonate	methylene glycol diformate
CH_4			5.53 ± 0.35
C_2H_6	2.67 ± 0.15		
C_3H_8	1.21 ± 0.06		
C_2H_4	1.78 ± 0.08		
CH_3OCHO		4.71 ± 0.70	
CH_2Cl_2			1.70 ± 0.10
C_2H_5Cl		0.96 ± 0.10	

TABLE 2: Measured Cl Atom Rate Constants ($cm^3 \text{ molecule}^{-1} s^{-1}$)

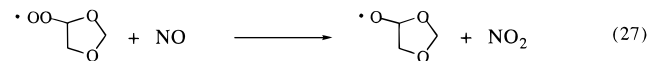
reference	reactant		
	1,3-dioxolane ($\times 10^{-10}$)	ethylene carbonate ($\times 10^{-12}$)	methylene glycol diformate ($\times 10^{-13}$)
CH_4			5.53 ± 0.35
C_2H_6	1.52 ± 0.09		
C_3H_8	1.69 ± 0.09		
C_2H_4	1.67 ± 0.08		
CH_3OCHO		6.59 ± 0.98	
CH_2Cl_2			5.61 ± 0.33
C_2H_5Cl		7.68 ± 0.77	

$= (1.63 \pm 0.20) \times 10^{-10}$, $k_{15} = (7.1 \pm 1.5) \times 10^{-12}$, and $k_{16} = (5.6 \pm 0.4) \times 10^{-13} \text{ cm}^3 \text{ molecule}^{-1} s^{-1}$. We estimate that potential systematic errors associated with uncertainties in the reference rate constants could add an additional 10% to the uncertainty range. Propagating this additional 10% uncertainty gives $k_{12} = (1.6 \pm 0.3) \times 10^{-10}$, $k_{15} = (7.1 \pm 1.7) \times 10^{-12}$, and $k_{16} = (5.6 \pm 0.7) \times 10^{-13} \text{ cm}^3 \text{ molecule}^{-1} s^{-1}$. Our result for k_{16} is in good agreement with the value of $k_{16} = (5.1 \pm 1.0) \times 10^{-13} \text{ cm}^3 \text{ molecule}^{-1} s^{-1}$ reported previously.¹¹ There are no literature data for k_{12} or k_{15} to compare with our results.

3.4. Mechanistic Study of 1,3-Dioxolane Oxidation at Wuppertal and Ford. The atmospheric oxidation of 1,3-dioxolane proceeds via OH radical attack which gives two different alkyl radicals.



In 1 atm of air, these alkyl radicals add O_2 to give peroxy radicals which react with NO to produce alkoxy radicals.



The alkoxy radicals will either react with O_2 to give cyclic carbonyl compounds or undergo ring-opening bond scission leading to the formation of linear multifunctional compounds. To provide an accurate description of the atmospheric chemistry of 1,3-dioxolane, we need information concerning the relative importance of attack by OH radicals on the two different

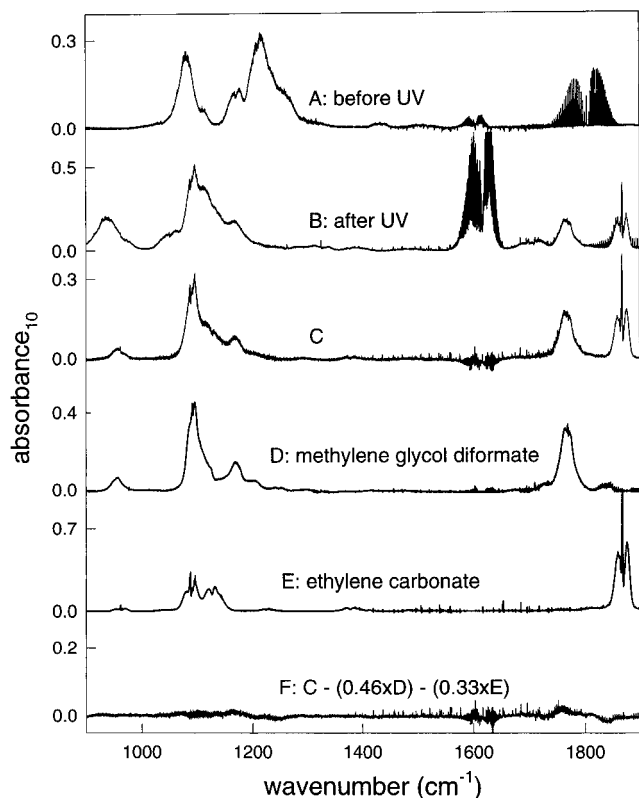


Figure 4. IR spectra acquired before (A) and after (B) a 20 s irradiation of a mixture of 18.7 mTorr of 1,3-dioxolane, 16.3 mTorr of NO, 96 mTorr of Cl₂, and 249 Torr of O₂ in 700 Torr total pressure of N₂ diluent. During the irradiation, 23% of the 1,3-dioxolane was consumed. Subtraction of features attributable to 1,3-dioxolane, NO, NO₂, HNO₃, and HONO from panel B gives panel C. Panels D and E show reference spectra of methylene glycol diformate and ethylene carbonate, respectively. Subtraction of the infrared features attributable to methylene glycol diformate and ethylene carbonate from panel C gives panel F.

—CH₂— groups and the fates of the corresponding alkoxy radicals. To provide such data, experiments were performed using the FTIR—smog chamber systems at Wuppertal and Ford.

Experiments employed the UV irradiation of 1,3-dioxolane/CH₃ONO/NO and 1,3-dioxolane/Cl₂/NO mixtures in 1 atm of O₂/N₂ diluent at 298 ± 4 K. Figure 4 shows typical IR spectra acquired before (A) and after (B) a 20 s irradiation of a mixture of 18.7 mTorr of 1,3-dioxolane, 16.3 mTorr of NO, 96 mTorr of Cl₂, and 249 Torr of O₂ in 700 Torr total pressure of N₂ diluent. During the irradiation, 23% of the 1,3-dioxolane was consumed. Subtraction of features attributable to 1,3-dioxolane, NO, NO₂, HNO₃, and HONO from panel B gives panel C. Panels D and E show reference spectra of methylene glycol diformate and ethylene carbonate, respectively, which are subtracted from the product spectrum in panel C. As shown in panel F, there are no products other than methylene glycol diformate and ethylene carbonate formed.

For the Cl-initiated reactions, the concentration of methylene glycol diformate and ethylene carbonate increased linearly with the loss of 1,3-dioxolane over the range of 1,3-dioxolane consumptions used (6–70%). After each experiment, the mixture was left to stand in the dark for about 10 min to measure the loss rate of ethylene carbonate in the dark and hence calculate appropriate corrections.¹⁷ Such corrections were in the range 2–5%. No changes in the ethylene carbonate and methylene glycol diformate yields were observed when the initial NO and Cl₂ concentrations were varied independently by factors of 5 and 2, respectively. For the OH-initiated

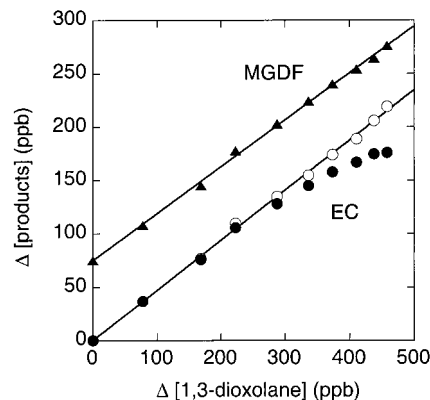
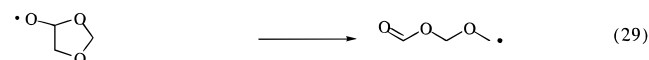


Figure 5. Formation of methylene glycol diformate MGDF (▲) and ethylene carbonate (EC), measured (●) and corrected for wall loss (○), versus loss of 1,3-dioxolane for an experiment using 1.34 ppm of 1,3-dioxolane, 4.6 ppm of methyl nitrite, 1.9 ppm of NO, and 206 mbar of O₂ in 1000 mbar total pressure of N₂ diluent at 297 K. The methylene glycol diformate data are shifted vertically by 75 ppb for clarity.

reactions, the concentration of methylene glycol diformate increased linearly with the loss of 1,3-dioxolane over the range of 1,3-dioxolane consumptions used (2–52%). The corresponding plot for ethylene carbonate shows curvature (Figure 5) due to deposition to the reactor walls. The curvature is minor for short irradiation times and was not observed in the chlorine-initiated experiments which employed shorter irradiation times. Correction¹⁷ of the observed ethylene carbonate concentrations for wall loss results in a linear increase of the ethylene carbonate production with the loss of 1,3-dioxolane. The yields of ethylene carbonate and methylene glycol diformate were independent of O₂ partial pressure over the range studied (60–800 mbar).

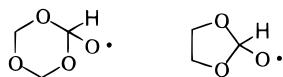
The observed molar yields of ethylene carbonate and methylene glycol diformate were 0.48 ± 0.07 and 0.50 ± 0.14 for OH radical initiation and 0.43 ± 0.07 and 0.53 ± 0.07 for Cl atom initiation. It should be noted at this point that Cl atom initiated oxidation of 1,3-dioxolane produces HO₂ radicals which react with NO to form OH radicals. Thus, in the Cl-initiated experiments there may be a contribution from OH radicals. Experiments involving 1,3-dioxolane have been performed previously in the EUPHORE outdoor smog chamber facility.¹⁸ Mixtures of 2 ppm of 1,3-dioxolane and 100–200 ppb of NO_x in air were prepared in the 168 m³ Teflon EUPHORE chamber and exposed to sunlight. Molar yields of (0.42 ± 0.10) for both ethylene carbonate and methylene glycol diformate were obtained from the EUPHORE experiments.¹⁸ The results from the present study are consistent with the outdoor smog chamber studies.

The observation of ethylene carbonate and methylene glycol diformate in yields which are independent of [O₂] over the range 60–800 mbar and account for 100% of the loss of 1,3-dioxolane serves to define the atmospheric oxidation mechanism. The absence of any effect of [O₂] shows that there is only one fate of each of the alkoxy radicals. Alkoxy radicals produced in reaction 25 react with O₂, while those formed in reaction 27 decompose.



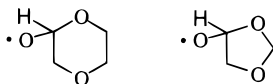
It is interesting to compare the behavior of the alkoxy radical derived from 1,3,5-trioxane with the analogous alkoxy radical

formed from 1,3-dioxolane. As shown below, the structures of the two alkoxy radicals are similar.



However, the atmospheric fates of these radicals are very different. There are two possible fates of these radicals: decomposition or reaction with O_2 . Under atmospheric conditions, the alkoxy radical derived from 1,3,5-trioxane undergoes essentially 100% ring opening decomposition via C–O bond scission. In contrast, the corresponding alkoxy radicals derived from 1,3-dioxolane react with O_2 to form ethylene carbonate. It is interesting that the relative importance of decomposition and reaction with O_2 changes so dramatically for these species. The cause of this change in behavior probably lies in the energetics associated with the decomposition reaction. A computational study of the energetics of these systems would be interesting but is beyond the scope of the present study.

The behavior of the other alkoxy radical derived from 1,3-dioxolane can be compared to the corresponding alkoxy radical formed in the oxidation of 1,4-dioxane.



The structures of these two alkoxy radicals are similar, and their atmospheric fate is the same, decomposition via C–C bond scission.^{19,20} The preference of these two radicals for decomposition via C–C bond scission rather than C–O bond scission or reaction with O_2 can be rationalized by their relatively low C–C bond strengths (decomposition results in the loss of a C–C bond and the formation of a C–O bond). This behavior is entirely consistent with the available database concerning the behavior of similar alkoxy radicals. Thus, decomposition via C–C bond scission has been shown to be the major fate of alkoxy radicals α to oxygen atoms in the ether linkages in diethyl ether,²¹ 2-ethoxy ethanol,²² and 2-butoxy ethanol.²³ The alkyl radical formed in reaction 29, $HC(O)OCH_2OCH_2\cdot$, reacts further to give methylene glycol diformate, $HC(O)OCH_2OCHO$.



The observation of stoichiometric conversion of $HC(O)OCH_2OCH_2\cdot$ radicals into methylene glycol diformate in the present work is consistent with the recent work in our laboratories showing that the atmospheric oxidation of 1,3,5-trioxane produces essentially 100% yield of methylene glycol diformate.¹¹

3.5. Cl Atom Initiated Oxidation of 1,3-Dioxolane in the Presence of NO_2 at Wuppertal. The UV irradiation of 1,3-dioxolane/ $Cl_2/NO/O_2/N_2$ mixtures resulted in consumption of NO and formation of ethylene carbonate, methylene glycol diformate, and NO_2 . When all of the NO had been consumed, additional product features at 792, 1300, 1726, and 1755 cm^{-1} were observed. The same IR product features were observed following irradiation of 1,3-dioxolane/ $Cl_2/NO_2/O_2$ mixtures. These features increased linearly with the consumption of 1,3-dioxolane and are ascribed to the formation of peroxy nitrates.



There was no discernible loss (<2%) of the peroxy nitrates on standing in the dark in the chamber for 10 min. However, addition of NO resulted in a complete (>95%) loss of the peroxy nitrates within the 2 min taken for the addition and the formation of approximately equal amounts of ethylene carbonate and methylene glycol diformate. The peroxy nitrates derived from 1,3-dioxolane are thermally unstable and decompose to give the peroxy radicals and NO_2 . In the presence of NO_2 , peroxy nitrate is reformed via reactions 33 and 34. Addition of NO serves to scavenge the peroxy radicals and prevents the reformation of the peroxy nitrate. The thermal stability of the peroxy nitrates derived from 1,3-dioxolane is low and, like other alkyl peroxy nitrates,⁶ will not play any role in atmospheric chemistry.

3.6. Chemical Modeling at Wuppertal. An explicit reaction mechanism for the OH-initiated degradation of 1,3-dioxolane in the presence of NO_x was developed using a simple box model.²⁴ The reaction scheme was checked by fitting the model to the experimental concentration–time profiles for 1,3-dioxolane, methylene glycol diformate, ethylene carbonate, NO, NO_2 , and methyl nitrite, simultaneously using 10 sets of experimental data with $[O_2] = 60\text{--}800$ mbar. The mechanism was based upon the RACM mechanism,²⁵ which is used widely to model the chemistry occurring in urban air. The RACM mechanism was modified by inclusion of the reactions describing CH_3ONO photolysis and 1,3-dioxolane degradation given in Table 3. The NO_2 photolysis rate ($J_{NO_2} = 3.76 \times 10^{-3} s^{-1}$) was measured in the Wuppertal chamber. The CH_3ONO photolysis rate cannot be obtained directly from the observed CH_3ONO decay since this compound is reformed by recombination of CH_3O radicals with NO. However, photolysis of CH_3ONO was the only OH source in the experiments and it was possible to obtain a value of $J_{CH_3ONO} = (0.95 \pm 0.17) \times 10^{-3} s^{-1}$ from a fit of the simulated VOC profiles to the experimental data. All other photolysis frequencies were evaluated relative to J_{NO_2} using the algorithm of Madronich.²⁶

The degradation scheme developed for 1,3-dioxolane is illustrated in Figure 6. The rate constants for the reactions of OH radicals with methylene glycol diformate and ethylene carbonate have not been measured and were estimated. Ethylene glycol diformate and dimethyl carbonate have molecular structures similar to those of methylene glycol diformate and ethylene carbonate and react with OH radicals with rate constants of $4.7 \times 10^{-13} s^{-1}$ ²⁰ and $3.2 \times 10^{-13} cm^3 molecule^{-1} s^{-1}$,²⁷ respectively. On the basis of these data, it seems reasonable to assume that the reactions of OH radicals with methylene glycol diformate and ethylene carbonate will proceed with rate constants of the order of $5 \times 10^{-13} cm^3 molecule^{-1} s^{-1}$. While such slow reactions will not play an important role in the present system, they were included in the mechanism for completeness. The observed wall loss for ethylene carbonate was also included in the model.

In the modeling exercise, the branching ratio of the initial reaction of OH with 1,3-dioxolane k_{1a}/k_{1b} and the nitrate from the reactions of peroxy radicals (RO_2 , $R'O_2$, and $HC(O)-(OCH_2)_2O_2$; see Table 3) with NO were varied to provide the best fit of the experimental data. The methylene glycol diformate and ethylene carbonate profiles were sensitive to the choice of k_{1a}/k_{1b} , while the NO and NO_2 profiles were sensitive to the

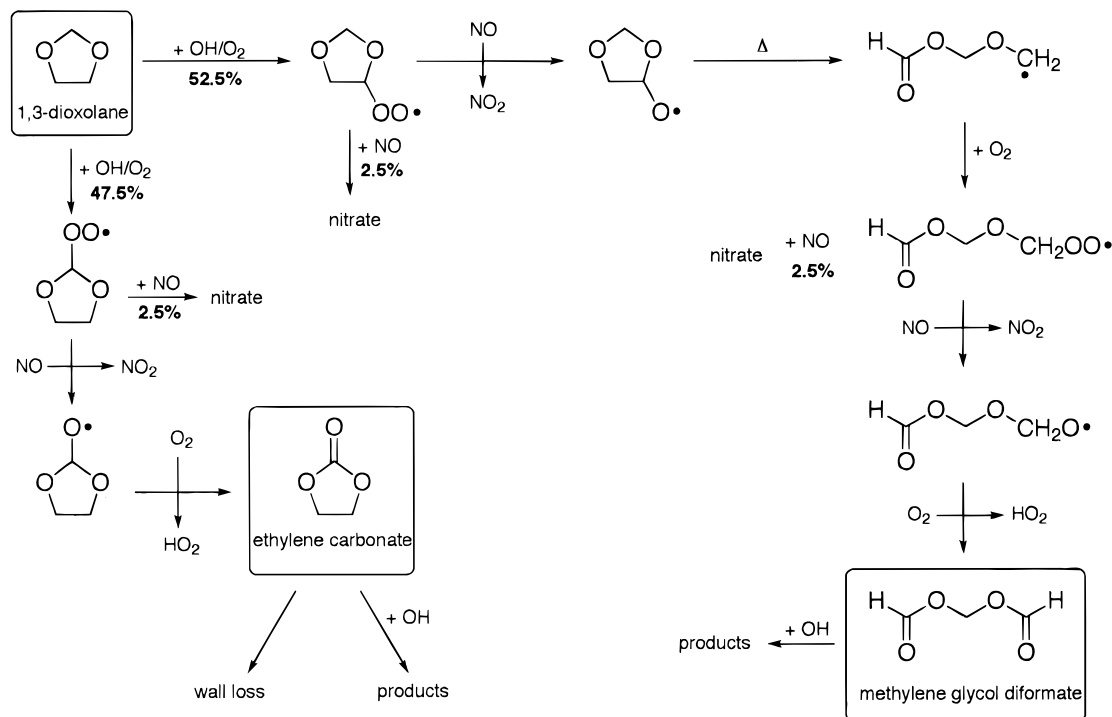
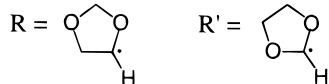


Figure 6. Degradation scheme for 1,3-dioxolane in the presence of NO_x .

TABLE 3: Chemical Mechanism Used in Simulations

reaction	k (298 K) ^a	ref
(a) Methyl Nitrite Chemistry		
$\text{CH}_3\text{ONO} + h\nu \rightarrow \text{CH}_3\text{O} + \text{NO}$	9.5×10^{-4}	this work
$\text{CH}_3\text{O} + \text{O}_2 \rightarrow \text{HCHO} + \text{HO}_2$	1.9×10^{-15}	14
$\text{HO}_2 + \text{NO} \rightarrow \text{OH} + \text{NO}_2$	8.1×10^{-12}	14
$\text{OH} + \text{CH}_3\text{ONO} \rightarrow \text{products}$	2.6×10^{-13}	31
$\text{OH} + \text{HCHO} \rightarrow \text{HCO} + \text{H}_2\text{O}$	1.0×10^{-11}	14
$\text{HCO} + \text{O}_2 \rightarrow \text{HO}_2 + \text{CO}$	5.5×10^{-12}	14
$\text{CH}_3\text{O} + \text{NO} \rightarrow \text{CH}_3\text{ONO}$	3.6×10^{-11}	14
$\text{CH}_3\text{O} + \text{NO} \rightarrow \text{HCHO} + \text{HNO}$	4.0×10^{-12}	14
$\text{CH}_3\text{O} + \text{NO}_2 \rightarrow \text{CH}_3\text{ONO}_2$	2.0×10^{-11}	14
(b) Degradation Scheme for 1,3-Dioxolane ^b		
$\text{OH} + 1,3\text{-dioxolane} \rightarrow \text{R} + \text{H}_2\text{O}$	5.4×10^{-12}	this work
$\text{R} + \text{O}_2 \rightarrow \text{RO}_2$	5.0×10^{-12}	estimated
$\text{RO}_2 + \text{NO} \rightarrow \text{RO} + \text{NO}_2$	1.0×10^{-11}	estimated
$\text{RO}_2 + \text{NO} \rightarrow \text{RONO}_2$	2.5×10^{-13}	this work
$\text{RO} \rightarrow \text{HC(O)(OCH}_2)_2$	4.2×10^5	estimated
$\text{HC(O)(OCH}_2)_2 + \text{O}_2 \rightarrow \text{HC(O)(OCH}_2)_2\text{O}_2$	5.0×10^{-12}	estimated
$\text{HC(O)(OCH}_2)_2\text{O}_2 + \text{NO} \rightarrow \text{HC(O)(OCH}_2)_2\text{O} + \text{NO}_2$	1.0×10^{-11}	estimated
$\text{HC(O)(OCH}_2)_2\text{O}_2 + \text{NO} \rightarrow \text{HC(O)(OCH}_2)_2\text{ONO}_2$	2.5×10^{-13}	this work
$\text{HC(O)(OCH}_2)_2\text{O} + \text{O}_2 \rightarrow \text{MGDF} + \text{HO}_2$	8.0×10^{-15}	estimated
$\text{OH} + 1,3\text{-dioxolane} \rightarrow \text{R}' + \text{H}_2\text{O}$	4.9×10^{-12}	this work
$\text{R}' + \text{O}_2 \rightarrow \text{R}'\text{O}_2$	5.0×10^{-12}	estimated
$\text{R}'\text{O}_2 + \text{NO} \rightarrow \text{R}'\text{O} + \text{NO}_2$	1.0×10^{-11}	estimated
$\text{R}'\text{O}_2 + \text{NO} \rightarrow \text{R}'\text{ONO}_2$	2.5×10^{-13}	this work
$\text{R}'\text{O} + \text{O}_2 \rightarrow \text{EC} + \text{HO}_2$	8.0×10^{-15}	estimated
$\text{EC} \rightarrow \text{wall loss}$	1.9×10^{-4}	this work
$\text{OH} + \text{EC} \rightarrow \text{products}$	5.0×10^{-13}	estimated
$\text{OH} + \text{MGDF} \rightarrow \text{products}$	5.0×10^{-13}	estimated

^a In units of $\text{cm}^3 \text{ molecule}^{-1} \text{ s}^{-1}$ (second order) or s^{-1} (first order). ^b MGDF = methylene glycol diformate; EC = ethylene carbonate.



nitrate yield. Nitrate yields in reactions of peroxy radicals with NO are generally determined by the size of the peroxy radical. Since the peroxy radicals formed during the oxidation of 1,3-dioxolane are all of a similar size, their nitrate yields were constrained to be equal. It was found that the best fits were achieved using $k_{1a}/k_{1b} = 47.5:52.5$ and with a nitrate formation

yield of 2.5% for reaction of NO with each of the peroxy radicals (RO_2 , $\text{R}'\text{O}_2$, and $\text{HC(O)(OCH}_2)_2\text{O}_2$; see Table 3). Figure 7 shows an example of the quality of the fits achieved. The ethylene carbonate concentration is underestimated slightly by the model for reaction times less than 14 min. This may be caused by the fact that the rate constant of the observed wall loss for ethylene

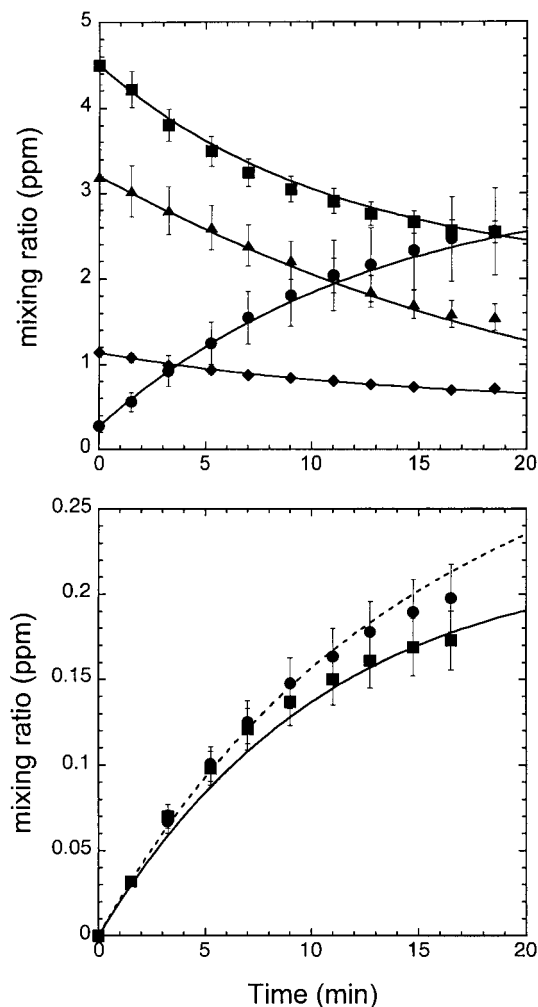


Figure 7. Comparison of experimental (symbols) and simulated (curves) concentration–time profiles. Top panel: 1,3-dioxolane (◆), CH₃ONO (▲), NO (■), and NO₂ (●). Bottom panel: ethylene carbonate (■) and methylene glycol diformate (●).

carbonate is weakly dependent on the reaction time. For the present computer simulations, an averaged value was used. For reaction times longer than 12 min, the modeled concentration of methylene glycol diformate is slightly higher than the experimental values. Nevertheless, the fact that within the experimental uncertainties the mechanism described above is able to account for the temporal changes of NO, NO₂, CH₃ONO, 1,3-dioxolane, ethylene carbonate, and methylene glycol diformate in the chamber demonstrates that we understand the chemical degradation mechanism of 1,3-dioxolane.

4. Conclusions

A substantial body of kinetic and mechanistic data pertaining to the atmospheric chemistry of 1,3-dioxolane is presented. It is expected that the atmospheric lifetime of 1,3-dioxolane is determined by reaction with OH radicals. While the OH radical concentration in the atmosphere varies with location, time of day, season, and meteorological conditions, a reasonable 24 h global average is $(0.5\text{--}1.0) \times 10^6$ molecules cm⁻³.^{28–30} At 295 K, the rate constant for reaction of OH radicals with 1,3-dioxolane is 8.8×10^{-12} cm³ molecule⁻¹ s⁻¹; hence, the atmospheric lifetime of 1,3-dioxolane will be 30–60 h. Reaction with OH gives two different alkyl radicals in approximately equal yield, which then add O₂ rapidly (within 1 μs) to give the peroxy radicals. In polluted urban air masses, the peroxy

radicals will react with NO within a few minutes leading to the formation of methylene glycol diformate and ethylene carbonate. Both species are relatively unreactive toward OH radicals and will not participate in further gas-phase reactions in urban airsheds.

Acknowledgment. We thank Bill Stockwell (Desert Research Institute) for sharing his computer code and for helpful discussions and Tobias Maurer (Bergische Universität GH Wuppertal) for a critical reading of the manuscript. Work at Wuppertal was funded by the EU and the German Bundesministerium für Bildung, Wissenschaft, Forschung und Technologie (BMBF), Project “Förderschwerpunkt Troposphärenforschung (TFS)”, Contract 07TFS30. T. J. Wallington acknowledges financial support by the Alexander von Humboldt Stiftung.

References and Notes

- (1) Roubi, M. A. *Chem. Eng.* **1995**, *44*, 37.
- (2) Hansen, K. B.; Wilbrandt, R.; Pagsberg, P. *Rev. Sci. Instrum.* **1979**, *50*, 1532.
- (3) Barnes, I.; Becker, K. H.; Mihalopoulos, N. *J. Atmos. Chem.* **1994**, *18*, 267.
- (4) Bierbach, A. Ph.D. Thesis, University of Wuppertal, Wuppertal, F.R.G., 1994.
- (5) Wallington, T. J.; Japar, S. M. *J. Atmos. Chem.* **1989**, *9*, 399.
- (6) Atkinson, R. *Chem. Rev.* **1986**, *86*, 69.
- (7) Horspool, W. M.; Song, P.-S., Eds. *CRC Handbook of Organic Photochemistry and Photobiology*; CRC Press: New York, 1995; p 337.
- (8) Field, N. D. *J. Am. Chem. Soc.* **1961**, *83*, 3504.
- (9) Posner, G. H.; Nelson, T. D. *Tetrahedron* **1990**, *46*, 4573.
- (10) Shaap, A. P. *Tetrahedron Lett.* **1971**, *21*, 1757.
- (11) Platz, J.; Christensen, L. K.; Sehested, J.; Nielsen, O. J.; Wallington, T. J.; Sauer, C.; Barnes, I.; Becker, K. H.; Vogt, R. *J. Phys. Chem. A* **1998**, *102*, 4829.
- (12) Nielsen, O. J.; Sidebottom, H. W.; Nelson, L.; Treacy, J. J.; O’Farrel, D. J. *Int. J. Chem. Kinet.* **1989**, *21*, 1101.
- (13) Atkinson, R. *J. Phys. Chem. Ref. Data* **1989**, Monograph 1.
- (14) DeMore, W. B.; Sander, S. P.; Golden, D. M.; Hampson, R. F.; Kurylo, M. J.; Howard, C. J.; Ravishankara, A. R.; Kolb, C. E.; Molina, M. J. *Jet Propulsion Laboratory Publication 97-4*; Pasadena, CA, 1997.
- (15) Wallington, T. J.; Hurley, M. D.; Ball, J. C.; Jenkin, M. E. *Chem. Phys. Lett.* **1993**, *211*, 41.
- (16) Wine, P. H.; Semmes, D. H. *J. Phys. Chem.* **1983**, *87*, 3572.
- (17) Atkinson, A.; Aschmann, S. M.; Carter, W. P. L.; Winer, A. M.; Pitts, J. N., Jr. *J. Phys. Chem.* **1982**, *86*, 4563.
- (18) Sauer, C. G.; Barnes, I.; Donner, B. In *The European Photoreactor, EUPHORE Report 1997*; Barnes, I., Wenger, J., Eds.; University of Wuppertal: Wuppertal, F.R.G., 1998; p 32.
- (19) Platz, J.; Sehested, J.; Møgelberg, T. E.; Nielsen, O. J.; Wallington, T. J. *J. Chem. Soc., Faraday Trans.* **1997**, *93*, 2855.
- (20) Maurer, T.; Hass, H.; Barnes, I.; Becker, K. H. *J. Phys. Chem. A*, submitted.
- (21) Wallington, T. J.; Japar, S. M. *Environ. Sci. Technol.* **1991**, *25*, 410.
- (22) Stemmler, K.; Mengon, W.; Kerr, J. A. *Environ. Sci. Technol.* **1996**, *30*, 3385.
- (23) Stemmler, K.; Mengon, W.; Kinnison, D. J.; Kerr, J. A. *Environ. Sci. Technol.* **1997**, *31*, 1496.
- (24) Seefeld, S.; Stockwell, W. R. *Atmos. Environ.*, in press.
- (25) Stockwell, W. R.; Kirchner, F.; Kuhn, M.; Seefeld, S. *J. Geophys. Res.* **1997**, *102*, 25847.
- (26) Madronich, S. *J. Geophys. Res.* **1987**, *92*, 9740.
- (27) Bilde, M.; Møgelberg, T. E.; Sehested, J.; Nielsen, O. J.; Wallington, T. J.; Hurley, M. D.; Japar, S. M.; Dill, M.; Orkin, V. L.; Buckley, T. J.; Huie, R. E.; Kurylo, M. J. *J. Phys. Chem. A* **1997**, *101*, 3514.
- (28) Ravishankara, A. R.; Lovejoy, E. R. *J. Chem. Soc., Faraday Trans.* **1994**, *90*, 2159.
- (29) Dorn, H.-P.; Brandenburger, U.; Brauers, T.; Ehhalt, D. H. *Geophys. Res. Lett.* **1996**, *23*, 2537.
- (30) Hofzumahaus, A.; Aschmutat, U.; Hessler, M.; Holland, F.; Ehhalt, D. H. *Geophys. Res. Lett.* **1996**, *23*, 2541.
- (31) Nielsen, O. J.; Sidebottom, H. W.; Donlon, M.; Treacy, J. *Int. J. Chem. Kinet.* **1991**, *23*, 1095.